Numerical modelling of viscoelastic waves by a pseudospectral domain decomposition method

Matt McDonald, Chris Bird and Michael Lamoureux

ABSTRACT

We present a method for numerically modelling viscoelastic wave propagation using domain decomposition combined with a pseudospectral method based on Legendre-Gauss-Lobatto nodes defined on a structured quadrilateral grid. The physics of the method is modelled using the Kelvin-Voigt equation for the time-dependent relation of stress and strain. Here we derive a coupled system of first-order equations for the particle velocities and accelerations which only doubles the number of required equations as opposed to the increase from 2 to 5 in the 2D case and 3 to 9 in the 3D case required when modelling the accelerations and stresses. Working with the first order system also allows us to incorporate absorbing boundary conditions by modifying the damping matrix at the boundary nodes in a way that further increases sparsity of the damping matrix and allows us to maintain the use of a low-storage explicit Runge-Kutta time-stepping algorithm.

INTRODUCTION

When a material is viscoelastic it means that the materials response to an applied stress is time-dependent, i.e. not instantaneous (Vasheghani and Lines, 2009; Carcione, 2001). What this means is that the strain of a viscoelastic material due to an applied stress is time delayed, the material has "memory" (Vasheghani and Lines, 2009). Viscoelastic behaviour is a prevalent feature in hydrocarbon reservoirs, for instance, heavy oils are viscoelastic (Vasheghani and Lines, 2009) and the ability to determine the viscosity in heavy oil reservoirs could greatly impact drilling programs and lead to the recovery of potentially stranded reserves (Vasheghani and Lines, 2009). The Kelvin-Voigt model for viscoelastic behaviour using springs and dash-pots is shown in figure . Here, E is the modulus of elasticity and η is the viscosity of the model.

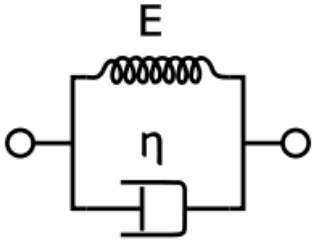

FIG. 1. Kelvin-Voigt spring and damper model.

The relationship between stress, σ, and strain, ε, is

$$\sigma = E\varepsilon + \eta\dot{\varepsilon},$$

where $\dot{\varepsilon}$ is the derivative with respect to time of the strain. In two spatial dimensions there are three independent stresses, $\{\sigma_{11}, \sigma_{22}, \sigma_{12}\}$, and strains $\{\varepsilon_{11}, \varepsilon_{22}, \varepsilon_{12}\}$. The strain

operator is defined

$$\varepsilon_{ij}(\mathbf{u}) = \frac{1}{2}\left(\partial_j u_i + \partial_i u_j\right)$$

where

$$\partial_i u_j = \frac{\partial u_j}{\partial x_i}$$

For an isotropic medium the stress-strain relation is the matrix equation

$$\begin{pmatrix}\sigma_{11}\\ \sigma_{22}\\ \sigma_{12}\end{pmatrix} = \begin{pmatrix}\lambda+2\mu & \lambda & 0\\ \lambda & \mu & 0\\ 0 & \lambda & \lambda+2\mu\end{pmatrix}\begin{pmatrix}\varepsilon_{11}\\ \varepsilon_{22}\\ \varepsilon_{12}\end{pmatrix}$$

$$+\begin{pmatrix}\lambda'+2\mu' & \lambda' & 0\\ \lambda' & \mu' & 0\\ 0 & \lambda' & \lambda'+2\mu'\end{pmatrix}\begin{pmatrix}\dot{\varepsilon}_{11}\\ \dot{\varepsilon}_{22}\\ \dot{\varepsilon}_{12}\end{pmatrix}$$

We can write this component-wise in terms of the vectors of displacements $\mathbf{u}$ and velocities $\mathbf{v}$ as

$$\sigma_{ij} = \lambda\nabla\cdot\mathbf{u}\delta_{ij} + 2\mu\varepsilon_{ij}(\mathbf{u}) + \lambda'\nabla\cdot\mathbf{v}\delta_{ij} + 2\mu'\varepsilon_{ij}(\mathbf{v}).$$

Assuming the displacements are of the form

$$u_j(x,z,t) = \hat{u}_j(x,z)e^{i\omega t}$$

produces

$$\begin{aligned}\sigma_{ij} &= \lambda\nabla\cdot\hat{\mathbf{u}}\delta_{ij} + 2\mu\varepsilon_{ij}(\hat{\mathbf{u}}) + i\omega\left(\lambda'\nabla\cdot\hat{\mathbf{u}}\delta_{ij} + 2\mu'\varepsilon_{ij}(\hat{\mathbf{u}})\right)\\ &= \Lambda\nabla\cdot\hat{\mathbf{u}}\delta_{ij} + 2M\varepsilon_{ij}(\hat{\mathbf{u}})\end{aligned}$$

where $\Lambda = \lambda + i\omega\lambda'$ and $M = \mu + i\omega\mu'$ are the complex Lamé parameters dependent on the frequency ω. This is the so-called correspondence principle, which assures that, for a given elastic model a viscoelastic counterpart is also available. Naturally then, the complex P and S wave velocities are defined as

$$\hat{V}_p = \sqrt{\frac{\Lambda+2M}{\rho}}, \quad \text{and} \quad \hat{V}_s = \sqrt{\frac{M}{\rho}}$$

The real velocities are obtained as

$$V_\alpha = \Re\left(\frac{1}{\hat{V}_\alpha}\right)^{-1}$$

where $\alpha = P$ or S. The frequency-dependent P and S wave quality factors are given by

$$Q_p = \frac{\lambda+2\mu}{\omega(\lambda'+2\mu')}, \quad \text{and} \quad Q_s = \frac{\mu}{\omega\mu'}.$$

Thus, we can obtain the elastic parameters, λ and μ as

$$\mu = \rho V_s^2 g(Q_s)$$

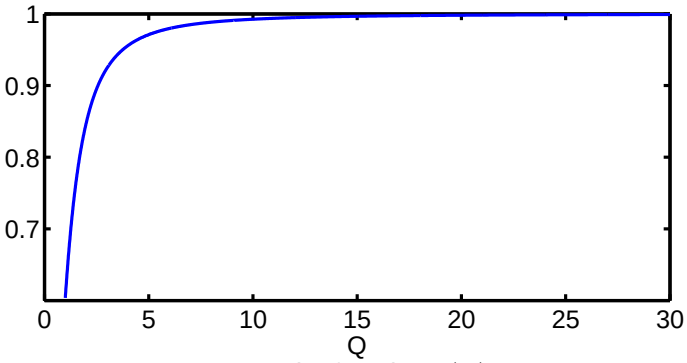

FIG. 2. The function $g(Q)$.

and

$$\lambda = \rho V_p^2 g(Q_p) - 2\mu$$

where g is obtained algebraically from the above equations as

$$g(Q) = \frac{1}{2}(1+Q^{-2})^{-1/2}(1+(1+Q^{-2})^{-1/2}).$$

The anelastic parameters are then obtained from

$$\lambda' = \frac{1}{\omega}\left(\frac{\lambda+2\mu}{Q_p} - \frac{2\mu}{Qs}\right)$$

and

$$\mu' = \frac{1}{\omega Q_s}.$$

The inputs of the model are thus ρ, V_p, V_s, Q_p and Q_s. The choice of ω is arbitrary but a good choice is generally the dominant frequency of the source wavelet

Further analysis of the anelastic properties of the model are available in (Carcione et al., 2004).

SPATIAL DISCRETIZATION

The strong-form of the equation of conservation of angular momentum can be written as

$$\rho\ddot{u}_i = \partial_j\sigma_{ij} + f_i, \quad \mathbf{x}\in\Omega, \quad t>0$$

where ρ is the density of the medium Ω, $\mathbf{x}$ is the vector of spatial variables and f_i is the i^{th} component of the applied force. Einstein's convention for summation over repeated indices is assumed.

To obtain the weak form we apply the method of Galerkin to obtain

$$\int_\Omega \rho\ddot{u}_i v d\Omega + \int_\Omega \sigma_{ij}(\mathbf{u})v_{,j}d\Omega = \int_\Omega f_i v d\Omega + \oint_\Gamma \sigma_{ij}(\mathbf{u})v\hat{n}_j d\Gamma. \tag{1}$$

The domain is then split up into several subdomains over which the integral is summed

$$\int_{\Omega_k} \rho\ddot{u}_i v d\Omega_k + \int_{\Omega_k} \sigma_{ij}(\mathbf{u})\partial_j v d\Omega_k = \int_{\Omega_k} f_i v d\Omega_k + \oint_{\Gamma_k} \sigma_{ij}(\mathbf{u})v\hat{n}_j d\Gamma_k. \tag{2}$$

Removing the boundary term at the inter-element boundaries enforces and continuous-stress interface condition. Removing it at a region boundary enforces a free-surface boundary condition allowing for the propagation of surface waves. At the artificial boundaries we impose the non-reflecting condition in (Stacey, 1988; Sochacki, 1988).

Referring the reader to our sister paper (McDonald et al., 2011), also found in this research collection, we omit the finer details of the element-wise discretization. The method is essentially to define a set of nodes on each element for which their is associated a set of pseudospectral differentiation matrices and integration weights. This allows us to replace differential operators with matrices and integration with a dot product. Pseudospectral methods can be made arbitrarily high-order in space by increasing the number of nodes in each element. Further, it is possible to define elements of different orders to correspond to portions of the medium where finer resolution is required.

TEMPORAL-DISCRETIZATION

Implementing the above spatial discretization results in the time-dependent system of equations for the nodal displacements in the k^{th} element,$\mathbf{u}_i^k(t)$,

$$M^k\ddot{\mathbf{u}}_i^k(t) + A_i^k\dot{\mathbf{u}}_i^k(t) + \sum_j \hat{K}_{ij}^k\dot{\mathbf{u}}_i^k(t) + \sum_j K_{ij}^k\mathbf{u}_j^k(t) = M^k\mathbf{f}_i^k(t).$$

M^k is the element mass matrix, A_i^k is the damping matrix corresponding to the absorbing boundary conditions applied to the i^{th} displacement, $\hat{K}_{ij}^k$ is the stiffness matrix associated with the viscoelastic term, K_{ij}^k is the stiffness matrix associated with the elastic term and $\mathbf{f}_i^k(t)$ is the vector of applied nodal forces. Note that the matrices A_i and $\hat{K}_{ij}^k$ have no overlapping entries and ultimately can be combined to form a single damping matrix that represents both the absorbing boundaries and the viscoelastic damping by editing the matrix $\hat{K}_{ij}^k$ to. For brevity we will simply denoted this combined absorbing/damping matrix as $\hat{K}_{ij}^k$.

The global system is then assembled using the so-called connectivity matrix as defined in our (McDonald et al., 2011). Where the viscoelastic case differs from the elastic case defined therein, is that the damping matrix is not diagonal and so the system cannot be numerically time-stepped using central finite differences without having to solve a large system of equations at each time step. Thus we must reduce the order of the system by doubling the number of equations.

Let $\mathbf{U}$ be the vector of nodal displacements ordered vertically

$$\mathbf{U} = [u_1(x_1, z_1, t), ..., u_1(x_n, z_n, t), u_2(x_1, z_1, t), ..., u_2(x_n, z_n, t)]^T.$$

Similarly let $\mathbf{V}$ be the vector of nodal velocities. The system is then re-written as

$$\begin{pmatrix} M & 0 \\ 0 & I \end{pmatrix}\begin{pmatrix} \dot{\mathbf{V}} \\ \dot{\mathbf{U}} \end{pmatrix} + \begin{pmatrix} \hat{K} & K \\ I & 0 \end{pmatrix}\begin{pmatrix} \mathbf{V} \\ \mathbf{U} \end{pmatrix} = \begin{pmatrix} \mathbf{F} \\ 0 \end{pmatrix}$$

We solve this by the 4^{th}-order low-storage explicit Runge-Kutta method (David and Ketcheson, 2010). These methods have the advantage over standard Runge-Kutta methods of

only requiring a single extra storage level, however, they must compute an additional intermediate step to update a single time-step. This is less of an issue than it may seem though as the resulting evolution equation is stable for larger time-steps than the standard methods.

CASE-STUDIES

We now present several thought experiments illustrating the use of our procedure. The source in each is a Ricker wavelet in time with dominant frequency $w_0 = 30$ applied at a single node at $x = 500$,$z = 0$. A free surface condition is enforced at $z = 0$ and absorbing boundaries are placed at the sides and bottom.

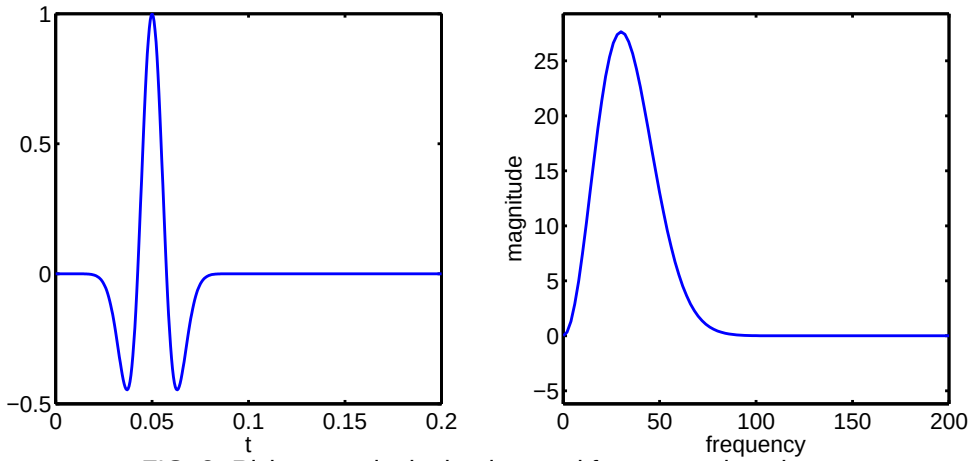

FIG. 3. Ricker wavelet in the time and frequency domains.

In the first we show the high-frequency damping present in the anelastic model by purposefully choosing a grid too coarse to represent the source wavelet. The model is 1000 meters by 1000 meters with $V_p = 2400$, $V_s = 1500$ and $\rho = 206$. From 0 to 250 meters the model is purely elastic with $Q_p = Q_s = \infty$, beyond that we add $Q_p = Q_s = 10$. We can see in figure 6 that as the source is propagated into the medium significant numerical dispersion is present. However, once the wave makes it to the anelastic region the high-frequency dispersion is damped considerably.

The second is the comparison of elastic and anelastic wave propagation. The elastic part of the model is the same as before. We compare the case of $Q_p = Q_s = \infty$, i.e a purely elastic medium, with $Q_s = 16$, and $Q_p = 24$. As we can see in figures 5 the wavelength in the anelastic media grows as the high-frequency portions of the wave is damped as it was in our first experiment.

In the third we again consider the case of an elastic-anelastic interface but this time are concerned with the reflection strictly from a difference in Q_p and Q_s. Using the data generated from this simple model of an elastic overburden overlaying a highly attenuative target, we wish to invert for Qp of the target. In order to achieve this there are two things which we require:

- A theoretical framework for the inversion of anelastic reflectivity, and

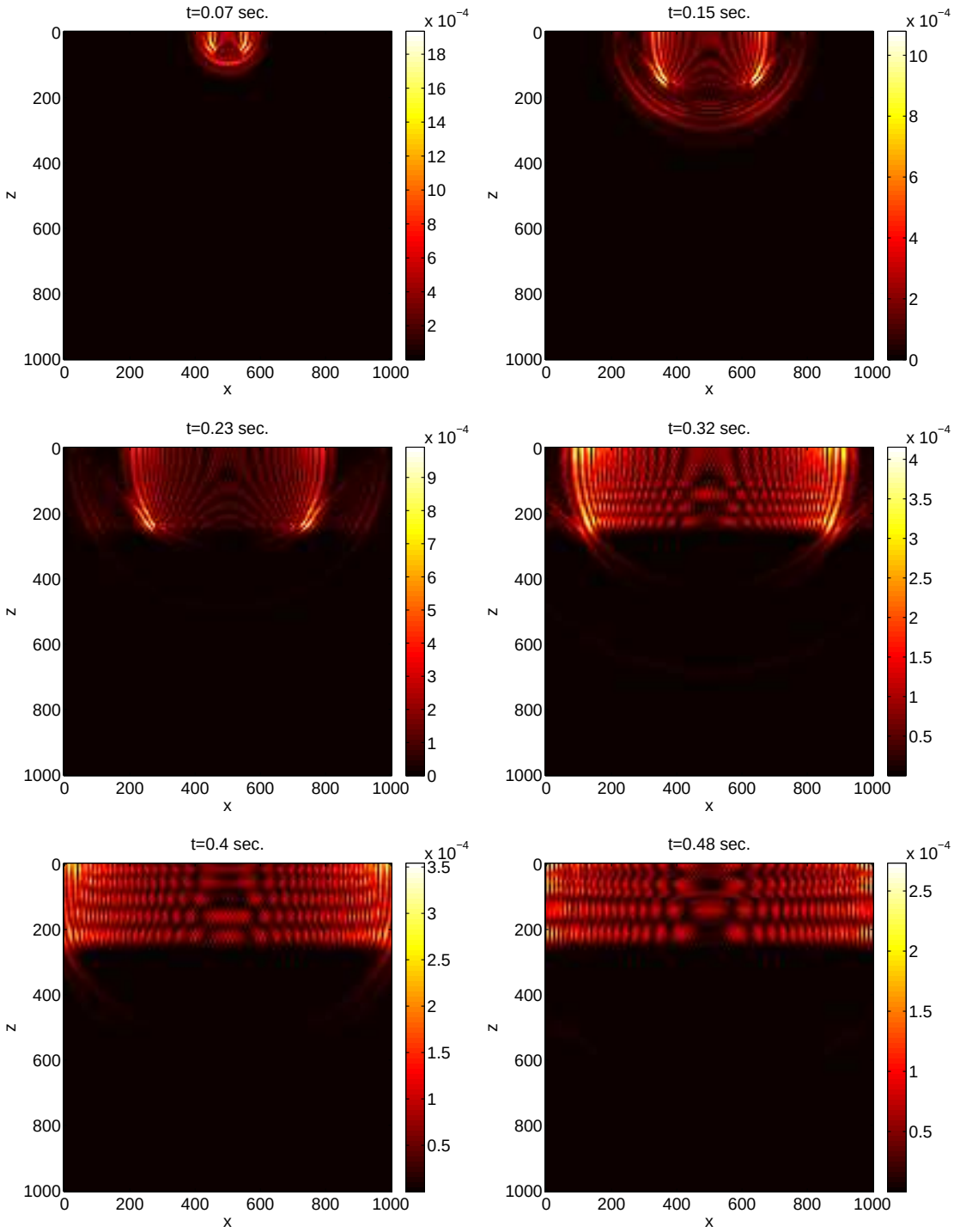

FIG. 4. Numerical dispersion damped by anelastic media

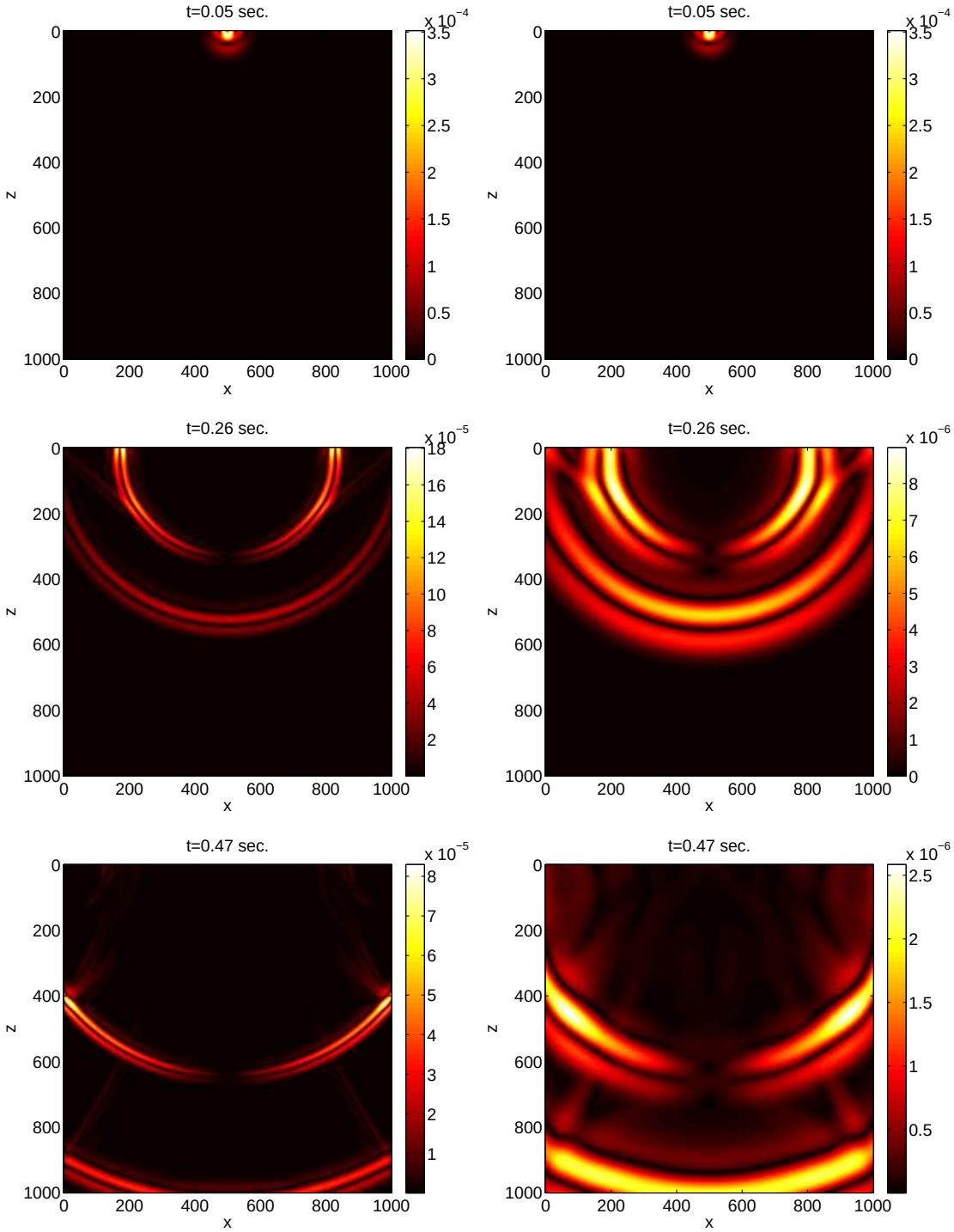

FIG. 5. Elastic vs. anelastic wave propagation.

- A method of time-frequency decomposition suitable for the extraction of the local spectra of seismic amplitudes

To meet this needs we have the following:

AVF inversion of anelastic reflectivity. One influence of Q on seismic reflection data is that a strong contrast in Q leads to a frequency dependent reflection coefficient (Lines et al., 2008; Innanen, 2011). An amplitude versus frequency (AVF) approach of inverting for Q from the frequency dependent reflection coefficient was developed by Innanen (2011). The method involves the difference of the dispersive reflection coefficient at two frequencies. For further details on AVF inversion see (Innanen, 2011; Bird et al., 2010a). We employ AVF inversion on our data generated for the elastic-anelastic model.

Fast S-transform. AVF inversion requires as input an estimate of the frequency dependent reflection coefficient. To meet this requirement we must employ a method of time-frequency decomposition. We have a calibrated, fast S-transform (FST) (Brown et al., 2010), which has been demonstrated to provide high fidelity estimates of the local spectra of seismic reflections (Bird et al., 2010b). Using the FST we may obtain an estimate of the local spectrum of the reflection from the elastic-anelastic interface and use as input for AVF inversion.

Inversion results

One final consideration before we may use the FST estimate of the spectrum of the absorptive reflection to invert for Q is that the modeling was performed with a wavelet. We must remove the influence of the wavelet on the spectrum of the reflection in order to invert for Q. There are two ways this could be done, Either the wavelet can be removed via deconvolution, or we can bring an estimate of the wavelet's spectrum into the inversion equations (Bird and Innanen, 2011). Because our data was modeled using a ricker wavelet, which is not minimum-phase, we cannot deconvolve the trace before inverting. Therefore, we bring the spectrum of the wavelet into the inversion framework and then invert for Q, for details on how this is done see Bird and Innanen (2011). Figure 8 shows the FST spectrum of the absorptive reflection (including the wavelet), this spectrum is used as input into the AVF inversion equations. The inverted value of Q we obtained was $Qp = 627$, which is much higher than the actual value of $Qp = 30$. Since AVF inversion has been shown to work accurately on deconvolved data (Bird et al., 2011), we believe that including the wavelet in the FST spectrum is the source of the error. As a topic of future work we will try a number of things to improve the accuracy of AVF inversion on this visco-elastic data including attempting the modelling using a minimum phase wavelet so that we may deconvolve the data before inverting or attempting to solve the problem of using FST, in the presence of wavelets, as input into AVF inversion.

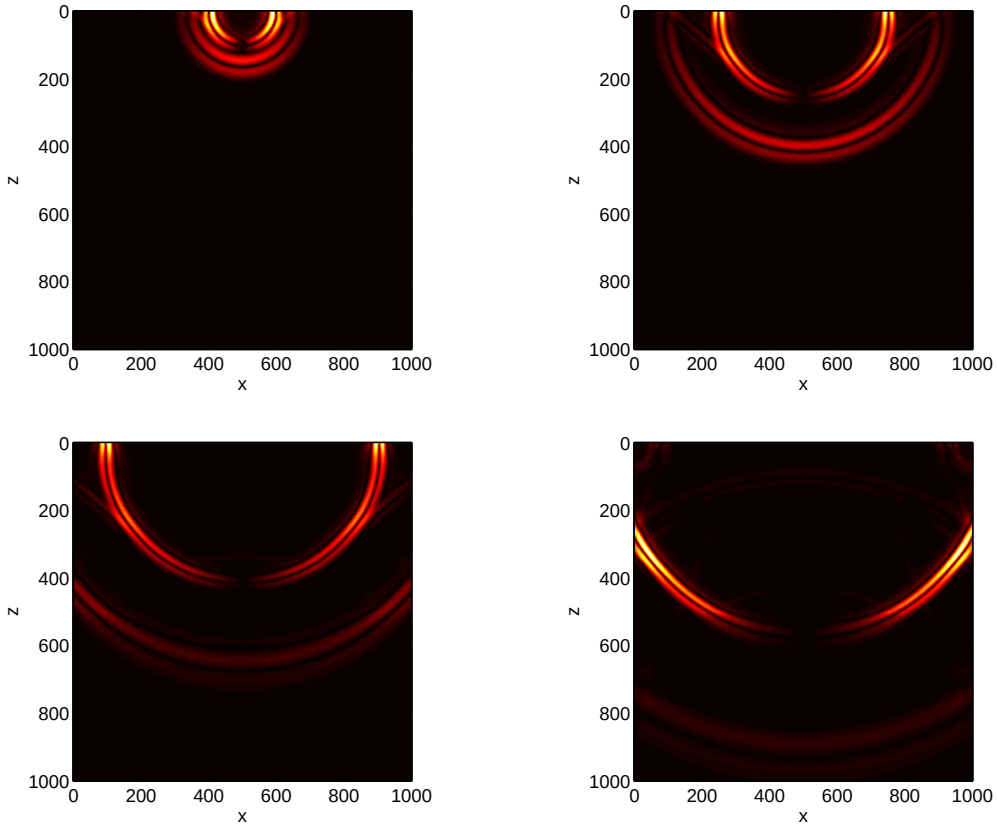

FIG. 6. Wave propagating through elastic-anelastic media.

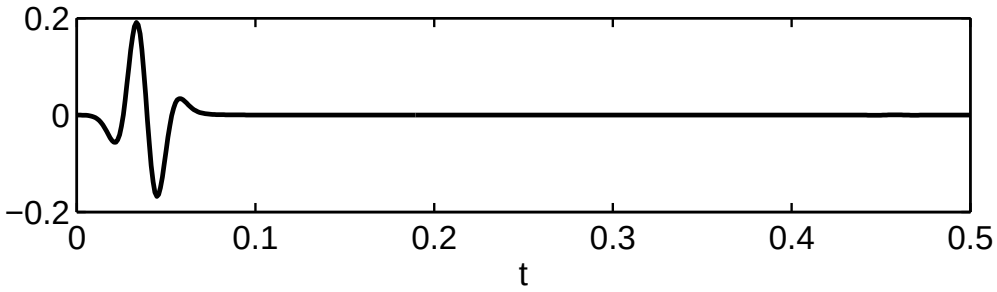

(a) Original trace.

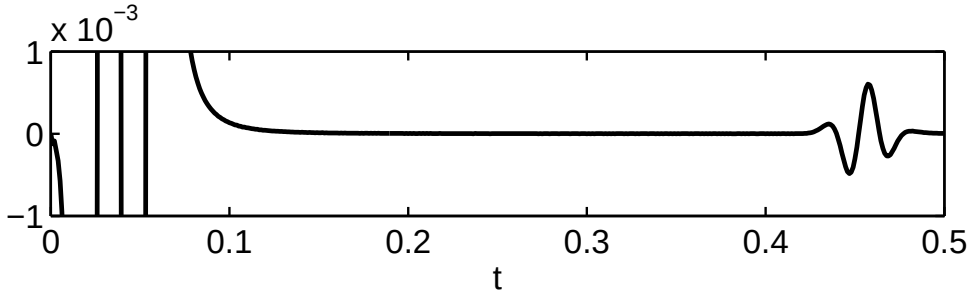

(b) Clipped trace.

FIG. 7. Zero-offset trace directly inline with source at surface showing reflection from Q.

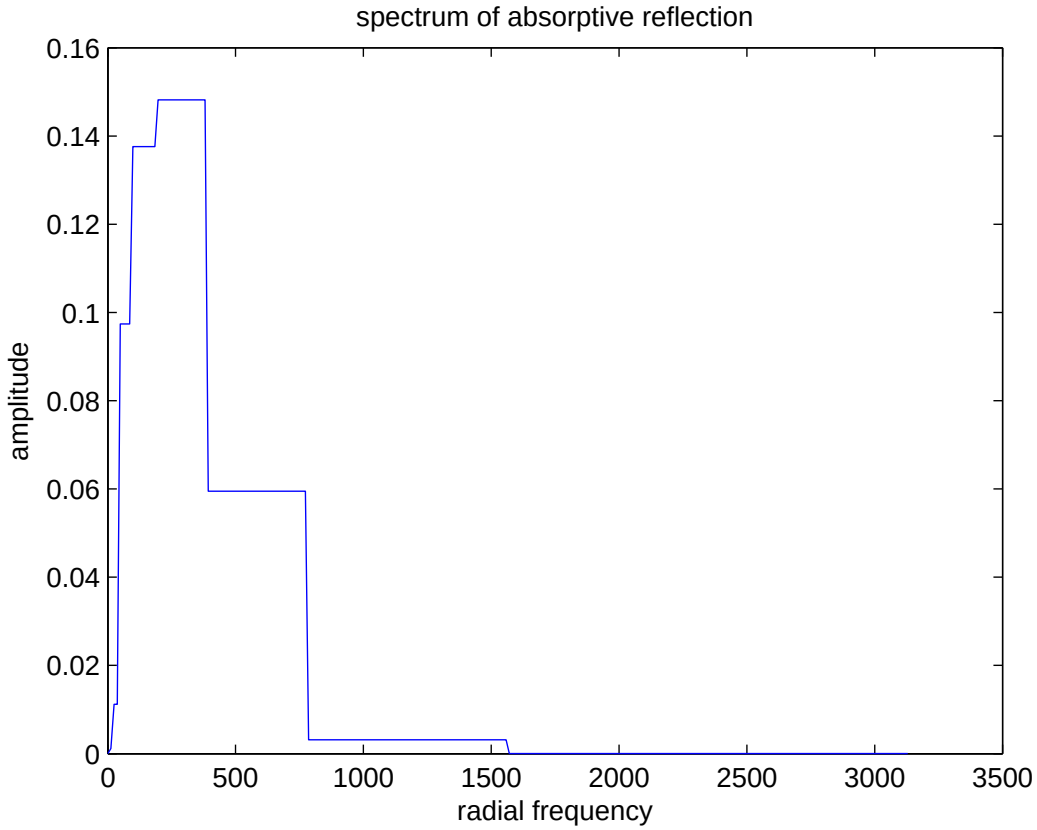

FIG. 8. FST spectrum of the absorptive reflection.

ACKNOWLEDGMENTS

We gratefully acknowledge the continued support of *mprime* through the POTSI research project and its industrial collaborators, the support of NSERC through the CREWES consortium and its industrial sponsors, and support of the Pacific Institute for the Mathematical Sciences.

REFERENCES

Bird, C., and Innanen, K., 2011, Least squares avf inversion: CREWES Sponsor's Meeting 2011, **23**, 1–10.

Bird, C., Innanen, K., Naghizadeh, M., and L, L., 2010a, Determination of anelastic reflectivity: how to extract seismic avf information: CREWES Annual Report, **22**, No. 4.

Bird, C., Innanen, K., Naghizadeh, M., and Lines, L., 2011, Avf inversion of anelastic reflectivity. practical issues concerning implementation.: CREWES Sponsor's Meeting 2011, **23**, 1–24.

Bird, C., Naghizadeh, M., and Innanen, K., 2010b, Amplitude calibration of a fast S-transform: CREWES Annual Report, **22**, 1–12.

Brown, R. A., Lauzon, M. L., and Frayne, R., 2010, A general description of linear time-frequency transforms and formulation of a fast, invertible transform that samples the continuous S-transform spectrum nonredundantly: IEEE Transactions on Signal Processing, **58**, No. 1, 281–290.

Carcione, J. M., 2001, Wave Fields in Real Media - Wave Propagation in Anisotropic, Anelastic and Porous Media: Elsevier.

Carcione, J. M., Poletto, F., and Gei, D., 2004, 3-d wave simulation in anelastic media using the kelvin-voigt constitutive equation: J. Comput. Phys., **196**, 282–297.

David, and Ketcheson, 2010, Runge kutta methods with minimum storage implementations: Journal of Computational Physics, **229**, No. 5, 1763 – 1773.

Innanen, K., 2011, Inversion of the seismic AVF/AVA signatures of highly attenuative targets: Geophysics, **76**, No. 1, R1–R14.

Lines, L., Vasheghani, F., and Treitel, S., 2008, Reflections on Q: CSEG Recorder, **December**, 36–38.

McDonald, M., Lamoureux, M., and Margrave, G., 2011, Pseudopectral-element modelling of elastic waves in matlab: CREWES Sponsor's Meeting 2011, **23**.

Sochacki, J., 1988, Absorbing boundary conditions for the elastic wave equations: Applied Mathematics and Computation, **28**, No. 1, 1 – 14.

Stacey, R., 1988, Improved transparent boundary formations for the elastic-wave equation: Bulletin of the Seismological Society of America, **78**, 2089–2097.

Vasheghani, F., and Lines, L. R., 2009, Viscosity and Q in heavy-oil reservoir characterization: The Leading Edge, **July**, 856–860.